

GAS ACCRETION ONTO GALACTIC DISCS IN COSMOLOGICAL SIMULATIONS OF GALAXY FORMATION

F.G. IZA¹, S.E. NUZA¹, C. SCANNAPIECO²

¹Instituto de Astronomía y Física del Espacio (CONICET-UBA) ² Departamento de Física (UBA)

INTRODUCTION

In the standard paradigm of galaxy formation and evolution, the baryonic component of galaxies forms from the collapse and condensation of gas within dark matter haloes, and later grows from continuous accretion of mass, both in diffuse form and in mergers with other systems. After a first period of rapid and violent halo growth, the gas settles into a rotationally-supported structure eventually giving rise to the formation of a stellar disc. Stars evolve and return chemically-processed gas and energy to the interstellar medium, mainly through Type II supernova explosions.

In the disc region, the cosmological accretion of gas combines with the outflows resulting from supernovae, affecting the hydrodynamical and structural properties of the disc and producing gas flows in the vertical and radial directions. Despite gas accretion is crucial for the evolution of the disc, it is only recently that this process has been studied in a cosmological context [1].

In this work, we use a simulation of the Auriga Project, a suite of magneto-hydrodynamical, zoom-in cosmological simulations of Milky Way-like galaxies, to study the temporal dependency of gas accretion onto the disc.

THE AURIGA PROJECT

The Auriga Project [2] is a suite of 30 high-resolution Milky Way-like galaxies simulated in a cosmological environment using the hydrodynamic code AREPO. All simulations follow the evolution of matter from $z = 127$ to $z = 0$ in a Λ CDM universe with $\Omega_0 = 0.307$, $\Omega_\Lambda = 0.693$ and a Hubble constant of $H_0 = 100 \text{ h km s}^{-1} \text{ Mpc}^{-1}$, where $h = 0.6777$. The simulated galaxies have $z = 0$ virial masses in the range $\sim 9 - 17 \times 10^{11} \text{ M}_\odot$ and stellar masses in the range $\sim 3 - 12 \times 10^{10} \text{ M}_\odot$.

The galaxy chosen for this analysis, labelled Au6, has been re-simulated with tracer particles in the gas component, which allows to follow the trajectories of gas particles across time. Fig. 1 shows the stellar (left) and gaseous (right) projected mass density distribution at $z = 0$ for Au6.

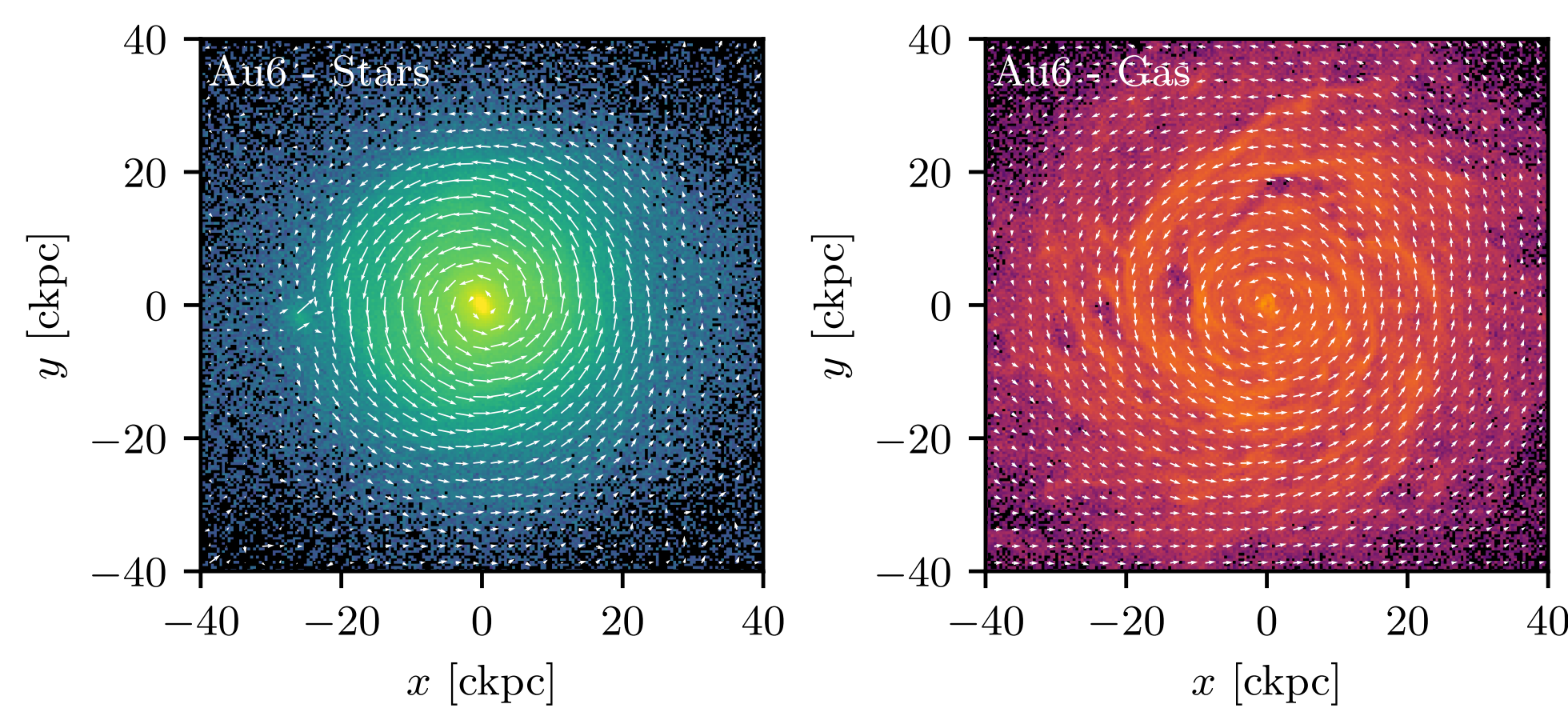


Figure 1: Face-on projected mass density distribution at $z = 0$ for stars (left panel) and gas (right panel).

REFERENCES

- [1] S.E. Nuza, C. Scannapieco, C. Chiappini, T.C. Junqueira, I. Minchev, and M. Martig, "Gas accretion in Milky Way-like galaxies: Temporal and radial dependencies," *Monthly Notices of the Royal Astronomical Society*, vol. 482, pp. 3089-3108, 2019.
- [2] R.J.J. Grand, F.A. Gómez, F. Marinacci, R. Pakmor, V. Springel, D.J.R. Campbell, C.S. Frenk, A. Jenkins, and S.D.M. White, "The Auriga Project: The properties and formation mechanisms of disc galaxies across cosmic time," *Monthly Notices of the Royal Astronomical Society*, vol. 467, pp. 179-207, 2017.

DEFINING THE DISC REGION

In order to compute the disc size (radius and height) at any given moment of the galactic evolution, and also to perform every subsequent analysis in this galaxy, we calculate the inertia tensor of the stars in the inner region of each halo and rotate the reference system in order to align the z -axis with the principal axis with the highest moment of inertia.

Subsequently, for each star particle in the galaxy, we calculate the circularity parameter $\epsilon = \frac{j_z}{j_{\text{circ}}}$, where $j_{\text{circ}} = r \sqrt{\frac{GM(r)}{r}}$ is the angular momentum expected for a circular orbit at the same radius. The disc radius r_d is then defined by the radius r_{xy} that encloses 90% of the total mass of stars with ϵ in the range $0.8 - 1.2$. In a similar fashion, we use this method to calculate the height above and below the disc plane. We show the evolution of these parameters in the bottom panels of Fig. 2: in the bottom-left panel we show the radius as a function of cosmic time and in the bottom-right panel we show the height of the disc as a function of cosmic time. In the latter, the positive curve indicates the height of the upper limit of the disc and vice versa. In red, we also show the values in physical coordinates.

Since the structure of the disc is of vital importance to galactic evolution, we also show in the figure below, the alignment between the gaseous and the stellar discs (top-left panel) and the disc-to-total mass fraction (top-right panel) as a function of cosmic time. In the latter, red dots indicate times when $D/T > 0.3$.

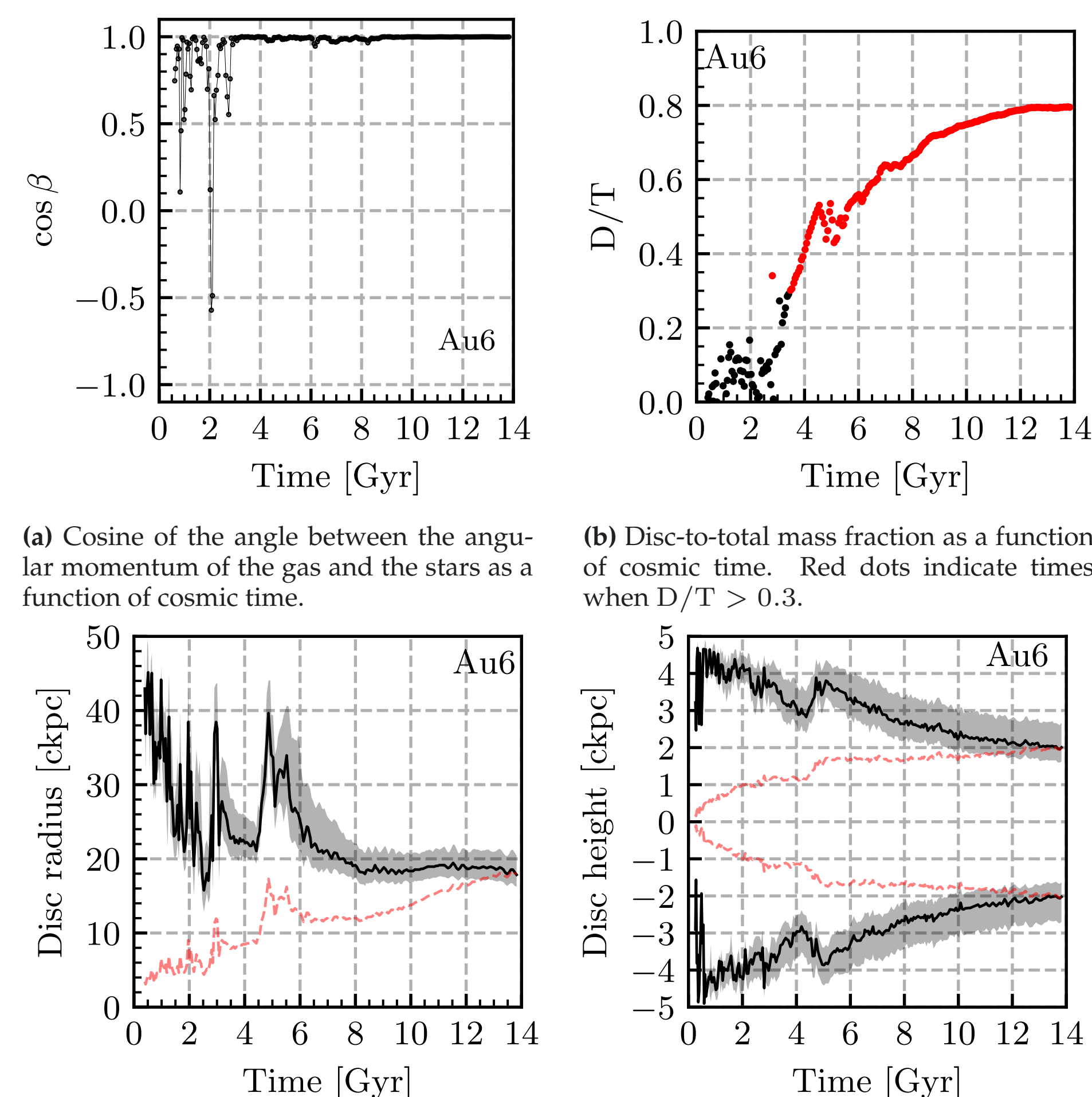


Figure 2: Evolution of disc properties (alignment, disc-to-total mass fraction, disc radius and disc height) as a function of time.

NET ACCRETION RATES

Fig. 3 shows the *net* accretion rate as a function of cosmic time for Au6. By definition, these values may be either positive (inflow-dominated times) or negative (outflow-dominated times). The black line shows the *positive* rates while the blue dots show *negative* rates in absolute value; note that outflow-dominated times are considerably less than the inflow-dominated times (30.5% versus 69.5%). Background shadows indicate the range of possible results obtained with the variation explained in the previous figure. The dashed black line is a non-linear least squares regression of the inflow-dominated times using the functional form

$$\dot{M}(t) = A \left(\frac{t}{t_0} \right)^\alpha \exp \left(-\frac{t}{t_0} \right).$$

This figure shows two distinct phases in the gaseous accretion of Au6:

- At early times, accretion rises abruptly following a power-law, and progressively slows down until it reaches a maximum value of $\sim 10 \text{ M}_\odot \text{ yr}^{-1}$ at $\sim 5 \text{ Gyr}$.
- After accretion reaches its maximum value, there is a second phase that lasts until the present, in which the accretion rate decreases exponentially with present-day values of $\sim 3 \text{ M}_\odot \text{ yr}^{-1}$.

INFLOW AND OUTFLOW RATE

The galaxy used in this study has been re-simulated in order to include gas tracer particles, whose trajectories can be followed in time. This is important because it allows us to separate accretion rates onto the disc in two components: *inflows* are composed by all the particles that fall into the disc at a certain time, while *outflows* are the particles that leave the disc (i.e., they were inside the disc in a previous time but are not in the present time).

Following a similar fashion as the previous box, the figure of the right shows these accretion rates: the black line indicates *inflows* and the blue line indicates *outflows*. It is important to distinguish between these accretion rates and the net accretion rate. First, *inflows* and *outflows* are, by definition, positive, while the *net* rate can be either positive or negative since it is computed subtracting the outflows from the inflows.

As with net accretion rates, the same two phases mentioned previously can be observed in the behaviour of the inflow/outflow rate. As expected, the values of inflow rate are in general greater than that of the net accretion, reaching a maximum value of $\sim 20 \text{ M}_\odot \text{ yr}^{-1}$ at $\sim 6 \text{ Gyr}$, while the outflow rate reaches its maximum of $\sim 10 \text{ M}_\odot \text{ yr}^{-1}$ at $\sim 8 \text{ Gyr}$. After this maximum, the inflow rate decays to a value of

The parameters obtained with the regression are $\alpha = 1.9 \pm 0.2$ and $t_0 = (2.6 \pm 0.3) \text{ Gyr}$. Note that α is the power-law exponent and t_0 is the characteristic time of the late-time exponential decay of accretion rates. The time at which the maximum value of the fitting function is reached is $\alpha t_0 = (4.9 \pm 0.8) \text{ Gyr}$.

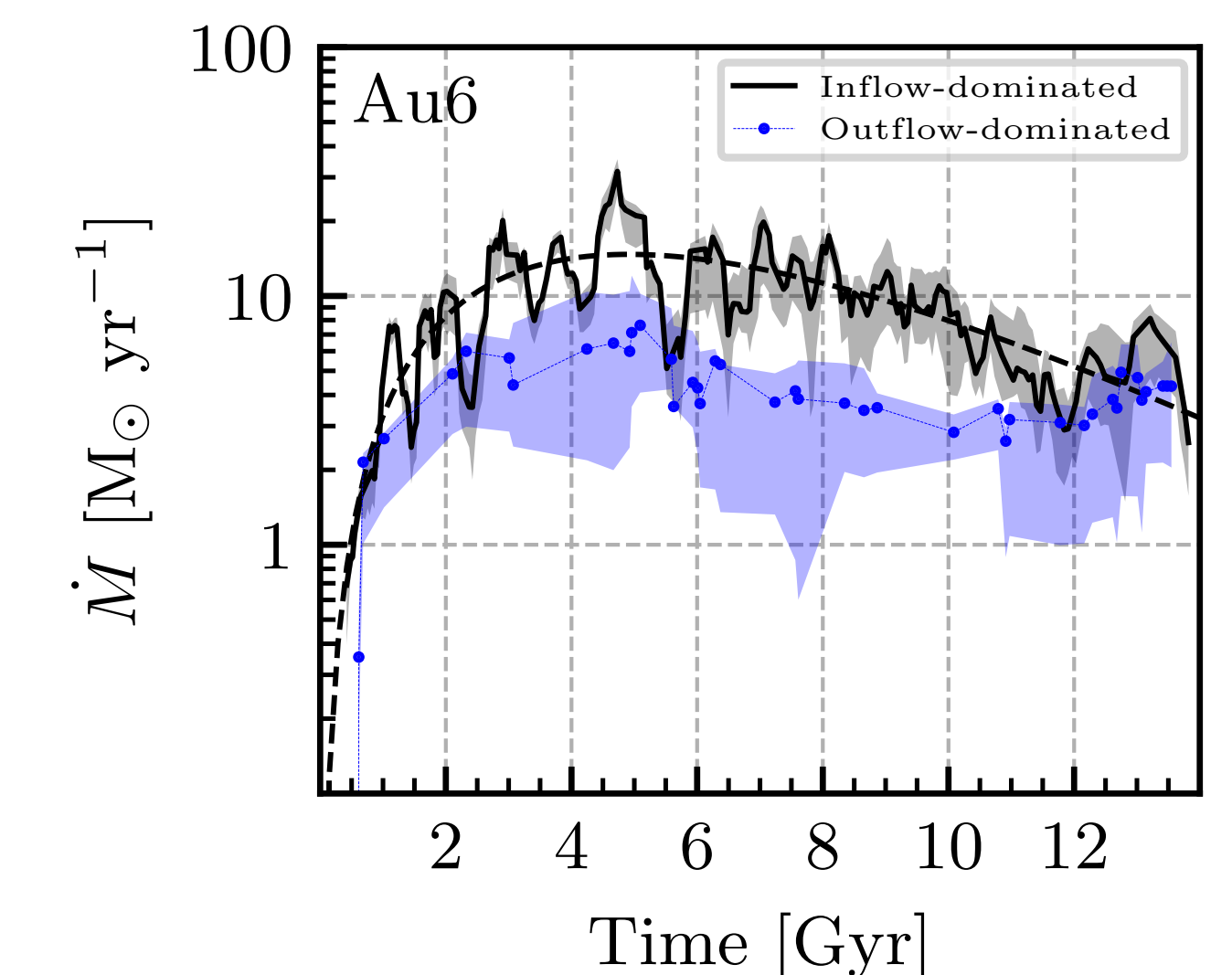


Figure 3: Net accretion rate as a function of time for Au6. The black line indicates the inflow-dominated times (positive net accretion) while blue dots indicate outflow-dominated times (negative net accretion) in absolute value. Grey and blue shadows indicate the variation of the accretion rates when the enclosed mass value used to define the disc varies between 85% and 95%. The dashed black line is the fit of the inflow-dominated times indicated in the text.

$\sim 10 \text{ M}_\odot \text{ yr}^{-1}$ at present times.

The parameters obtained with the regression are $\alpha_{\text{if}} = 1.8 \pm 0.2$ and $t_{0,\text{if}} = (3.4 \pm 0.3) \text{ Gyr}$ for inflows and $\alpha_{\text{of}} = 2.8 \pm 0.2$ and $t_{0,\text{of}} = (2.8 \pm 0.2) \text{ Gyr}$ for outflows. The time at which the maximum value of the fitting function is reached is $(6.1 \pm 0.9) \text{ Gyr}$ for inflows and $(7.8 \pm 0.8) \text{ Gyr}$ for outflows.

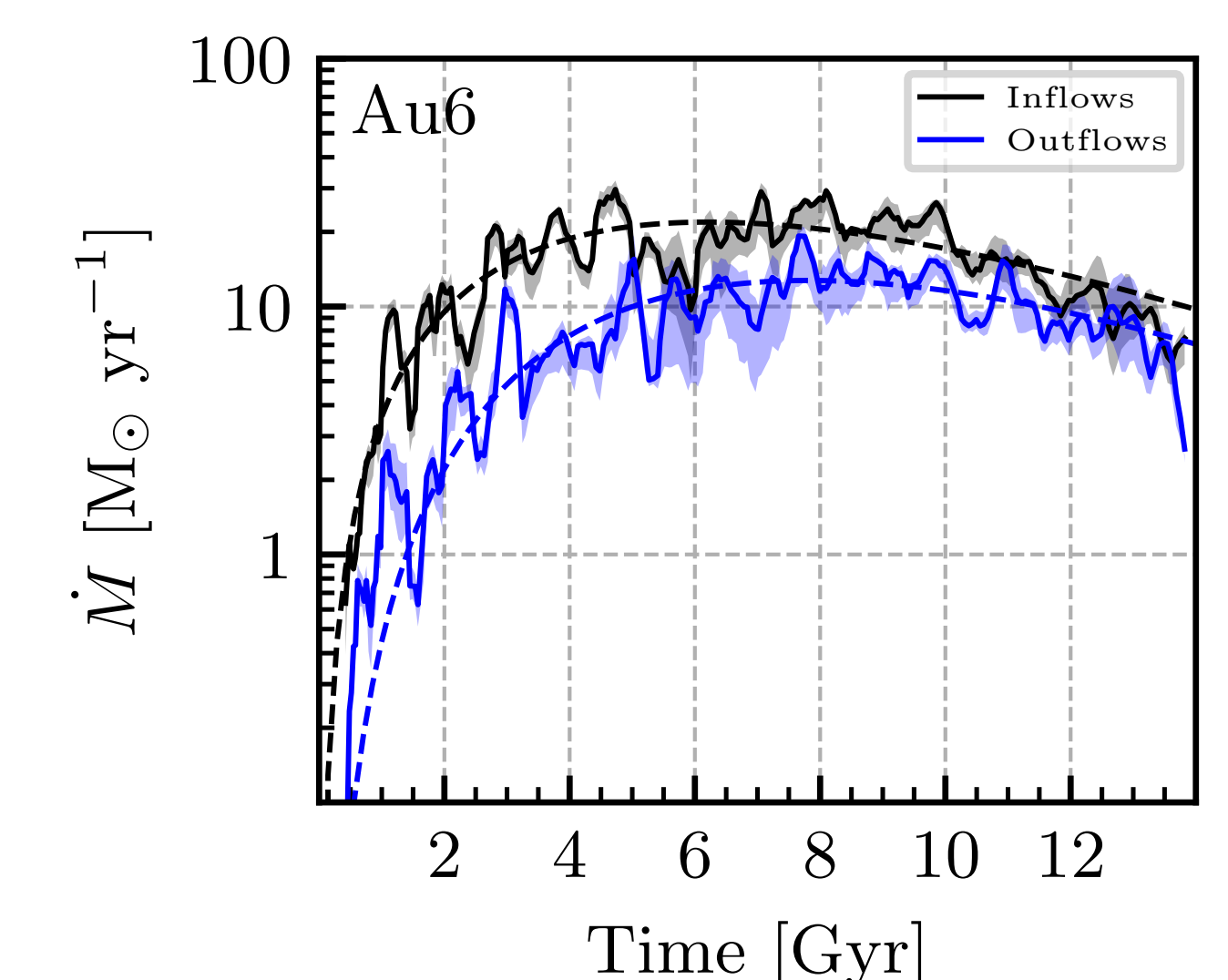


Figure 4: Inflow (black line) and outflow (blue line) accretion rates as a function of time for Au6. As before, shadows indicate the variation of the accretion rates when the enclosed mass value varies between 85% and 95%. Dashed lines are fits of the inflow (black) and outflow (blue) rates.

SUMMARY AND CONCLUSIONS

In this work, we presented an analysis of gas accretion onto the disc of a simulated galaxy from the Auriga Project. We found that inflows, outflows and net gas accretion rates follow a similar trend, with an early period when accretion rates rise abruptly before reaching their maximum values, and a second period characterised by a smooth decay until the

present.

This analysis will be extended to the full Auriga sample in order to quantify variations in the accretion rates of Milky-Way mass galaxies, expected in the context of a Λ CDM cosmology.